

Total-energy-based prediction of a quasicrystal structure

M. Mihalkovič^{1,2}, I. Al-Lehyani³, E. Cockayne⁴, C.L. Henley⁵, N. Moghadam⁶, J.A. Moriarty⁷, Y. Wang⁸, M. Widom³

¹ *Institute für Physik, Technische Universität Chemnitz, D-09107 Germany*

² *Institute of Physics, Slovak Academy of Sciences, Bratislava, Slovakia*

³ *Department of Physics, Carnegie Mellon University, Pittsburgh PA 15213*

⁴ *Ceramics Division, NIST, Gaithersburg MD 20899-8520*

⁵ *Department of Physics, Cornell University, Ithaca NY 14853*

⁶ *Oak Ridge National Laboratory, Oak Ridge TN 37831-6114*

⁷ *Lawrence Livermore National Laboratory, Livermore CA 94551*

⁸ *Pittsburgh Supercomputer Center, Pittsburgh PA 15213*

(April 26, 2024)

Abstract

Quasicrystals are metal alloys whose noncrystallographic symmetry and lack of structural periodicity challenge methods of experimental structure determination. Here we employ quantum-based total-energy calculations to predict the structure of a decagonal quasicrystal from first principles considerations. We employ Monte Carlo simulations, taking as input the knowledge that a decagonal phase occurs in Al-Ni-Co near a given composition, and using a few features of the experimental Patterson function. The resulting structure obeys a nearly deterministic decoration of tiles on a hierarchy of length scales related by powers of τ , the golden mean.

Al-Ni-Co forms thermodynamically stable and highly perfect decagonal quasicrystalline samples over a range of compositions [1]. Of special interest is the composition $\text{Al}_{0.70}\text{Ni}_{0.21}\text{Co}_{0.09}$ for which the structure is periodic along the z axis with a period of $c = 4.08 \text{ \AA}$, and quasiperiodic perpendicular to this axis with a characteristic length (termed a “quasilattice constant”) of $a_0 = 2.45 \text{ \AA}$ [2]. This “basic Ni” composition is well suited for theoretical modeling because it should be the simplest structure, lacking the quasiperiodic modulation and c -axis doubling observed at other compositions. Numerous attempts to determine the structure of this compound start from experimental data [3–5] but do not *predict* a structure on the basis of total energy.

The transition metals Ni and Co (generically denoted “TM”) play similar chemical roles in Al-transition metal quasicrystals, and they are not distinguished by ordinary X-ray or electron diffraction. Our model predicts distinct sites for Ni and Co near the “basic” composition.

Our total energy calculations employ quantum-based pair-potentials derived from the generalized pseudopotential theory (GPT) [6]. GPT expands the total energy in a series of volume-, pair- and many-body-potentials. The volume term exerts no force and may be neglected at fixed volume and composition. The many-body terms are small except among clusters of neighboring transition-metal atoms, and we incorporate their influence with modified short-ranged TM-TM pair interactions constrained by full *ab initio* calculations.

We identify four salient properties of the computed oscillatory potentials [6]: (1) $V_{\text{AlAl}}(r)$ has a broad shoulder starting around $r = 2.9 \text{ \AA}$ and is repulsive at shorter distances; (2) $V_{\text{AlCo}}(r)$ and $V_{\text{AlNi}}(r)$ exhibit deep first minima near $r = 2.5 \text{ \AA}$ and second minima near $r = 4.5 \text{ \AA}$; (3) The V_{AlCo} well is significantly deeper than the V_{AlNi} well; (4) The modified $V_{\text{TM-TM}}(r)$ have shallow minima near $r=2.6 \text{ \AA}$.

The following features of the $d(\text{AlNiCo})$ structures are evident in the experimentally determined Patterson function [3] which contains a peak at every interatomic vector \mathbf{r} : (A) All atoms lie on or nearly on layers separated by $c/2 = 2.04 \text{ \AA}$; (B) The vector from an atom to a nearest neighbor (with a tolerance of $\sim 0.1 \text{ \AA}$) belongs to a small, discrete basis set of

“linkage” vectors; (C) The in-plane components of linkage vectors are $\pm a_0 \mathbf{e}_i$ (see Fig. 1) or simple sums of such vectors.

We construct trial quasicrystal structures that achieve low total energy while satisfying the above experimental constraints. To enforce constraints (B) and (C) we limit atomic positions to a collection of discrete sites (Fig. 1), located at vertices of a two-dimensional tiling of rhombi with edge a_0 and acute angles 36° or 72° . To enforce constraint (A) we stack two independent tilings above each other. As the tiles can be placed in many ways, and atoms distributed randomly among the sites, these *minimal constraints* permit a great variety of structures, including all reasonable quasicrystal structures. After we discover favorable low energy motifs consistent with the minimal constraints, we remove unnecessary degrees of freedom, effectively defining *highly constrained* models.

A Metropolis Monte Carlo annealing yields low energy structures. Two kinds of Monte Carlo steps are employed: (i) swaps between nearby atoms of different species in either layer, including hops of one atom to an empty ideal site nearby; (ii) “flips” which reshuffle the three rhombi in a fat or thin hexagon, in one layer. (see Fig. 1) Due to the hexagon flips, our ensemble is an “equilibrium random tiling” allowing phason disorder [7], but the system is free to find a quasiperiodic state if that is favored by the potentials. Our simulations are performed with periodic boundary conditions using cell sizes chosen to best approximate the quasiperiodic structure.

In our initial simulation with minimal constraints, we employ a cell of size $12.22 \times 14.37 \times 4.08 \text{ \AA}^3$ and composition $\text{Al}_{34}\text{Ni}_{12}\text{Co}_4$. This cell contains 72 ideal sites, 36 in each layer with the c -axis periodicity enforced. Slow cooling identifies a unique minimum energy configuration illustrated in Fig. 2a.

The optimal configuration can be described simply in terms of a new *highly constrained* model (see Fig. 2b) that obeys the following rules: (i) the entire plane is tiled by three compound tiles called “hexagon”, “boat”, and “star”, outlined by heavy edges and built respectively of three, four, and five rhombi (this is called the “HBS” tiling [9]). (ii) The optimal decoration of the HBS tiles is virtually unique. Minimally constrained simulations

with larger cells support these rules.

We can understand this decoration in terms of the salient features of the potential we enumerated at the start. In view of features (1) and (2), the minimum-energy structure must maximize the number of Al-Co and Al-Ni bonds. In view of feature (3), every Co ought to have purely Al neighbors, which is geometrically feasible just up to $\sim 10\%$ Co, which is the “basic” composition. Thus, all TM-TM neighbors must be Ni-Ni. Every Ni has mostly Al neighbors but cannot escape having two or three Ni neighbors, since $\sim 30\%$ of all atoms are transition metals.

Let us check which ideal-site separations are favorable for which atom pairs. Within the same layer, the tile edge length $r_2=2.45 \text{ \AA}$ is unfavorable for Al-Al or TM-TM bonds, but highly favorable for Al-TM bonds. However, because of the high density of Al atoms, we find a small number of Al-Al bonds do take this length. The short diagonal of a fat rhombus is $r_3 = 2.88 \text{ \AA}$, which is an acceptable Al-Al distance. Hence the 72° Al-TM-Al isosceles triangle (half a fat rhombus) is highly favored within a layer.

The interlayer spacing $c/2=2.04 \text{ \AA}$ is too short for any pair. Sites in adjacent layers, spaced by $\tau^{-1}a_0$ in-plane (e.g., the short diagonal of the thin rhombus), are separated by $r'_1 = 2.54 \text{ \AA}$ which is favorable for Al-TM or TM-TM bonds. Finally, sites in adjacent layers separated by a_0 in-plane have a total separation of $r'_2 = 3.19 \text{ \AA}$ which is an acceptable Al-Al distance.

Given this understanding of chemical bond lengths we can easily justify the decoration of the HBS tiles. Each tile is bounded by Al atoms of alternating heights at separation r'_2 . Interior sites of the hexagon tile are too close to the Al border for Al atoms. Since it must hold two TM atoms, it holds a pair of Ni atoms at distances r'_1 and r_2 from the border Al and mutual separation r'_1 . Four of the border Al atoms form a rectangle with edges r'_2 and r_3 lying in a plane that is nearly the perpendicular bisector of the Ni-Ni bond. This fragment of the hexagon tile is thus a slightly distorted region of B2 (CsCl) structure [10].

The interior vertex of the boat and star tiles are at the ideal TM distance r_2 from border Al atoms. Since this is a point of high Al coordination, it is occupied by Co. The boat and

star tiles have room for two additional interior Al atoms at separation r_3 . In an isolated star tile this interior Al pair can lie in any of five symmetry-related configurations. The structure surrounding the star generally breaks this degeneracy by means of long-range interactions.

In the decoration just described, an Al atom on an HBS tiling vertex is often at the center of a small cluster which was an important motif of earlier models [8,9]. This cluster appears in Fig. 2b wherever hexagons join at their tips. This cluster consists of a pentagon of mixed Al and Ni atoms in the same layer as the vertex Al, and additional pentagons in the adjacent layers above and below. These adjacent pentagons contain only Al atoms and are rotated by 36° with respect to the middle pentagon. This cluster exhibits interlayer Al-Ni separations of 2.54 \AA and 4.46 \AA , precisely at the first and second minima of V_{AlNi} .

Since the HBS tile corners are all multiples of 72° , edges emanating from the HBS corner atoms in one layer can only point in the five directions $+\mathbf{e}_i$ while those within the other layer point in the directions $-\mathbf{e}_i$. Statistically, the layers are equivalent but related by a screw axis. Allowing for the reflection planes normal to the layers, and in the absence of further symmetry-breaking, the HBS decoration implies a space group $10_5/mmc$, consistent with experiment.

For the next level of modeling, we take the highly constrained HBS tiles as fundamental objects. Tile-tile interactions are defined implicitly as the sum of the pair potentials between atoms decorating the tiles. The allowed “flips” (Monte Carlo moves) of the HBS tiling are called “bow tie flips” as the tile edges before and after the flip outline a bow tie shape [9]. The bow tie flips are generated by fat hexagon flips of the underlying rhombus tiling. Additionally the Al pair inside the star can rotate among its five allowed orientations. The reduced degrees of freedom make the highly constrained HBS tiling much faster to simulate at low temperatures than the minimally constrained rhombus tiling.

The ensemble of random HBS tilings contains a variable tile frequency ratio H:B:S because HS pairs interchange with BB pairs by bow tie flips. Highly constrained simulations forbid this flip because it alters the chemical composition, given our ideal tile decoration. There is a particular “golden” ratio $H:B:S = \sqrt{5}\tau : \sqrt{5} : 1$ that is obtained, for example, by

removing double-arrow edges from a Penrose tiling. Decorating such a tiling deterministically yields an ideal composition $\text{Al}_{0.700}\text{Ni}_{0.207}\text{Co}_{0.093}$ and atomic volume 14.16 \AA^3 . Both composition and atomic volume are consistent with experiment.

Large-scale simulations (see Fig. 3) reveal a “supertile” ordering in which hexagons connect tip-to-tip. Each hexagon tip becomes a vertex of a “supertiling”, with longer edges of length $\tau^2 a_0$ along the midline of every hexagon. Since orientations of adjoining hexagons differ by multiples of 72° degrees, the same is true for their midlines, hence the “supertile” edges differ by 72° angles and form mainly HBS tiles (as well as a new “defect” tile).

The supertile atomic structure is mechanically stable. Under relaxation of the structure shown in figure 2 (which consists of two large scale hexagons), the average Co and Ni displacement is just 0.10 \AA . The average Al displacement is 0.17 \AA except for the two Al atoms located slightly off-center in the large-scale hexagons which displace 1.13 \AA to the symmetric points at the hexagon centers.

The “defect” tile breaks the connectivity of the small-hexagon chain, introducing a new tile shape which we call a “bow tie”. To understand the role of the bow tie and its low symmetry decoration, consider the energetics of the large scale HBS tilings. Because the large-scale HBS tile decoration is essentially deterministic, we may replace the actual interatomic interactions with effective interactions between tiles. We find a single parameter dominates the energetics: an energy cost is associated with 72° junctions between tile edges decorated with Ni atom pairs, because the resulting high density of Ni atoms reduces the number of favorable Al-Ni bonds. Defect tiles enter only when they reduce the number of 72° junctions. They accomplish this reduction by interchanging a NiNi pair with a nearby AlCo pair.

An alternate means of reducing the frequency of 72° angles between tile edges decorated with Ni atom pairs is to alter the chemical composition. To accommodate the new composition we must relax certain constraints in our simulation. We keep the small scale HBS tiles with Al fixed on their boundaries, but allow arbitrary chemical occupancy of the interior sites. Replacing 20 % of NiNi pairs with AlCo pairs eliminates all defects from the minimum

energy configuration and leads to chemical composition $\text{Al}_{0.720}\text{Ni}_{0.166}\text{Co}_{0.114}$, still within the limits of the basic Ni composition. The low energy configurations consist entirely of HBS tiles decorated as found previously, but now many tile edges that participate in two 72° junctions get decorated with an AlCo pair rather than a NiNi pair (see Fig. 3b).

We compare our model with experimental Z-contrast electron microscope imagery [5]. This experimental method images atomic columns proportionally to the mean square atomic number of the column, so the images translate quite directly into TM positions. A key feature of the experimental data is the occurrence of decagonal rings with a 20 \AA diameter. These rings exhibit up to 10 TM doublets around the perimeter, an interior ring of 10 TM singlets, and a central triangular core [5]. This characteristic structure is in excellent agreement with our model, where two hexagons and a boat frequently coalesce into a decagonal cluster (see center of Fig. 3b). The triangular core of this cluster, which breaks decagonal symmetry, is recognized as the sail of the boat tile. Full *ab-initio* calculations [11] recently verified energetic favorability of this particular core structure.

Our study began with interatomic potentials plus a minimum of experimental information. We derived structural models starting with a minimally constrained lattice gas on a fluctuating rhombus tiling. Systematically removing unnecessary degrees of freedom yielded a nearly deterministic decoration of HBS tiles at a length scale τ^2 times larger than the initial rhombus tiling, a model consistent with Z-contrast electron microscopy. This procedure can be repeated to identify yet larger characteristic atomic clusters providing a novel example of multiscale modeling which might be applicable to other quasicrystals.

This research was supported by the National Science Foundation and the Department of Energy.

REFERENCES

- [1] Ritsch, S., *et al.*, *Phil. Mag. Lett.* **78**,67-76 (1998).
- [2] Ritsch, S., *et al.*, *Phil. Mag. Lett.*, **74**, 99-106 (1996); Tsai, A.P., Fujiwara, A., Inoue, A. and Masumoto, T., *Phil. Mag. Lett.*, **74** 233-40 (1996).
- [3] Steurer, W., Haibach, T., Zhang, B., Kek, S. and Lück, R., *Acta Cryst. B* **49**, 661-75 (1993).
- [4] Yamamoto, A. and Weber, S., *Phys. Rev. Lett.*, 4430-3 **78** (1997); Steinhardt, P.J., *et al.*, *Nature* **396**, 55-7 (1998); Krajčí, M., Hafner, J. and Mihalkovič, M., *Phys. Rev. B* **62**, 243-55 (2000).
- [5] Abe, E., *et al.*, *Phys. Rev. Lett.* **84** 4609-12 (2000); Yan, Y., Pennycook, S.J. and Tsai A.P., *Phys. Rev. Lett.* **81**, 5145-8 (1998).
- [6] Moriarty, J.A. and Widom, M., *Phys. Rev. B* **56**, 7905-17 (1997); Al-Lehyani, I., *et al.*, cond-mat/0010205, submitted to *Phys. Rev. B* (2000).
- [7] Henley, C.L., “Random tiling models” in *Quasicrystals: The state of the art*, ed. D.P. DiVincenzo and P.J. Steinhardt, (World Scientific, Singapore, 1991) p. 429
- [8] Burkov, S.E., *Phys. Rev. Lett.* **67**, 614-17 (1993).
- [9] Cockayne, E. and Widom, M., *Phys. Rev. Lett.* **81**, 598-601 (1998).
- [10] W. Steurer, *Mat. Sci. Eng. A* **294-296**, 268-271 (2000).
- [11] Y. Yan and S.J. Pennycook, *Phys. Rev. Lett.* **86**, 1542-1545 (2001).

TABLES

Label	Example	Comments
$r_1=1.51 \text{ \AA}$	$a_0(\mathbf{e}_0 + \mathbf{e}_3)$	Forbidden
$r_2=2.45 \text{ \AA}$	$a_0\mathbf{e}_0$	Al-TM, (Al-Al)
$r'_1=2.54 \text{ \AA}$	$a_0(\mathbf{e}_0 + \mathbf{e}_3) + \frac{c}{2}\hat{z}$	Al-TM, TM-TM
$r_3=2.88 \text{ \AA}$	$a_0(\mathbf{e}_1 - \mathbf{e}_0)$	Al-Al
$r'_2=3.19 \text{ \AA}$	$a_0\mathbf{e}_0 + \frac{c}{2}\hat{z}$	Al-Al

TABLE I. Characteristic distances (illustrated in Fig. 1) and important bond types. Primed vectors connect adjacent layers.

FIGURES

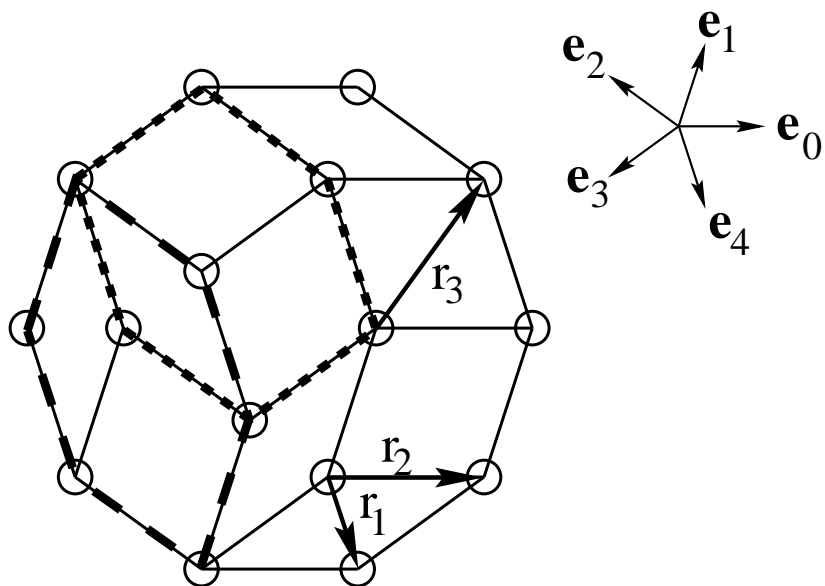


FIG. 1. Random rhombus tiling decorated with ideal sites. The long- and short-dashed lines outline, respectively, thin and fat hexagons. Unit vectors $\{\mathbf{e}_i\}$ lie parallel to tile edges. Vectors \mathbf{r}_i are defined in the table.

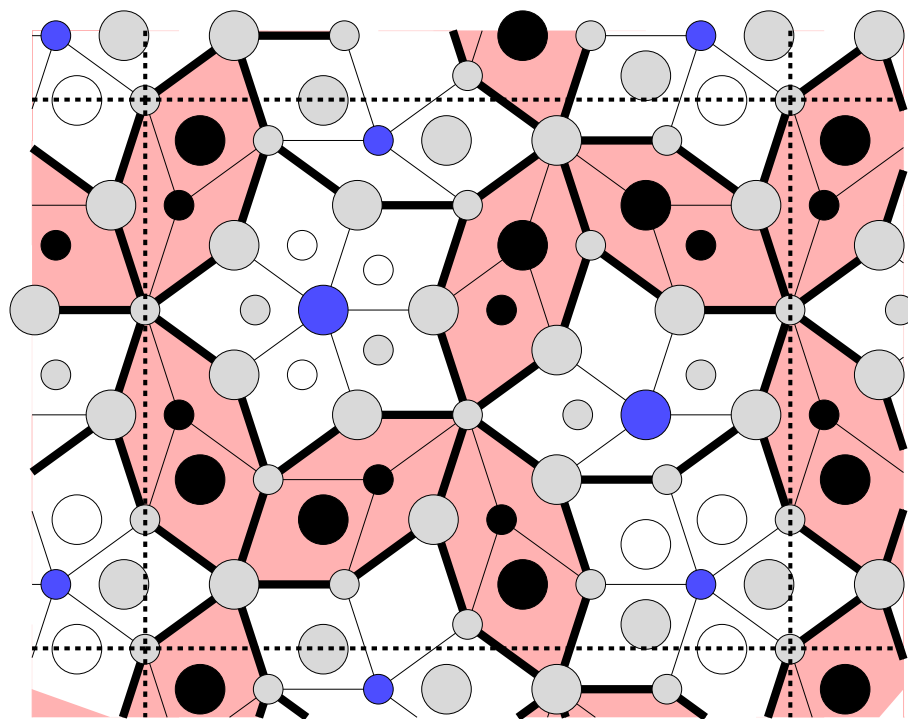
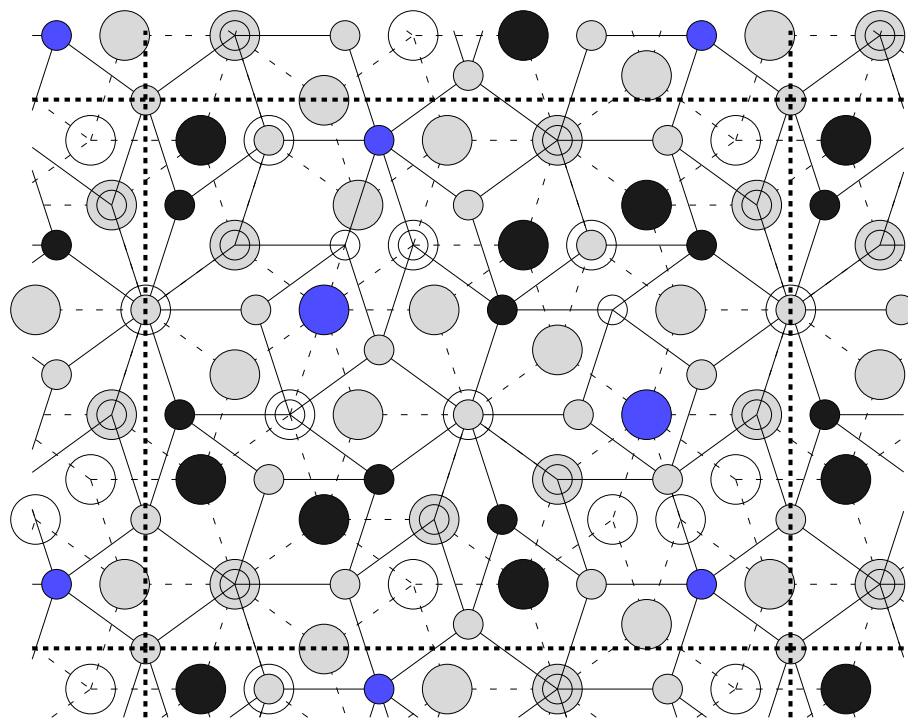


FIG. 2. Minimum energy configurations. Small/large circles indicate atoms in upper/lower layer. Gray=Al, Blue=Co, Black=Ni, White=vacant. (a) Top figure results from minimally constrained simulation (solid/dashed lines denote upper/lower tilings). (b) Bottom figure results from highly constrained simulation. Dark solid lines outline a_0 -scale HBS tiling. Pink-shaded hexagons connect vertices of $\tau^2 a_0$ -scale HBS tiling.

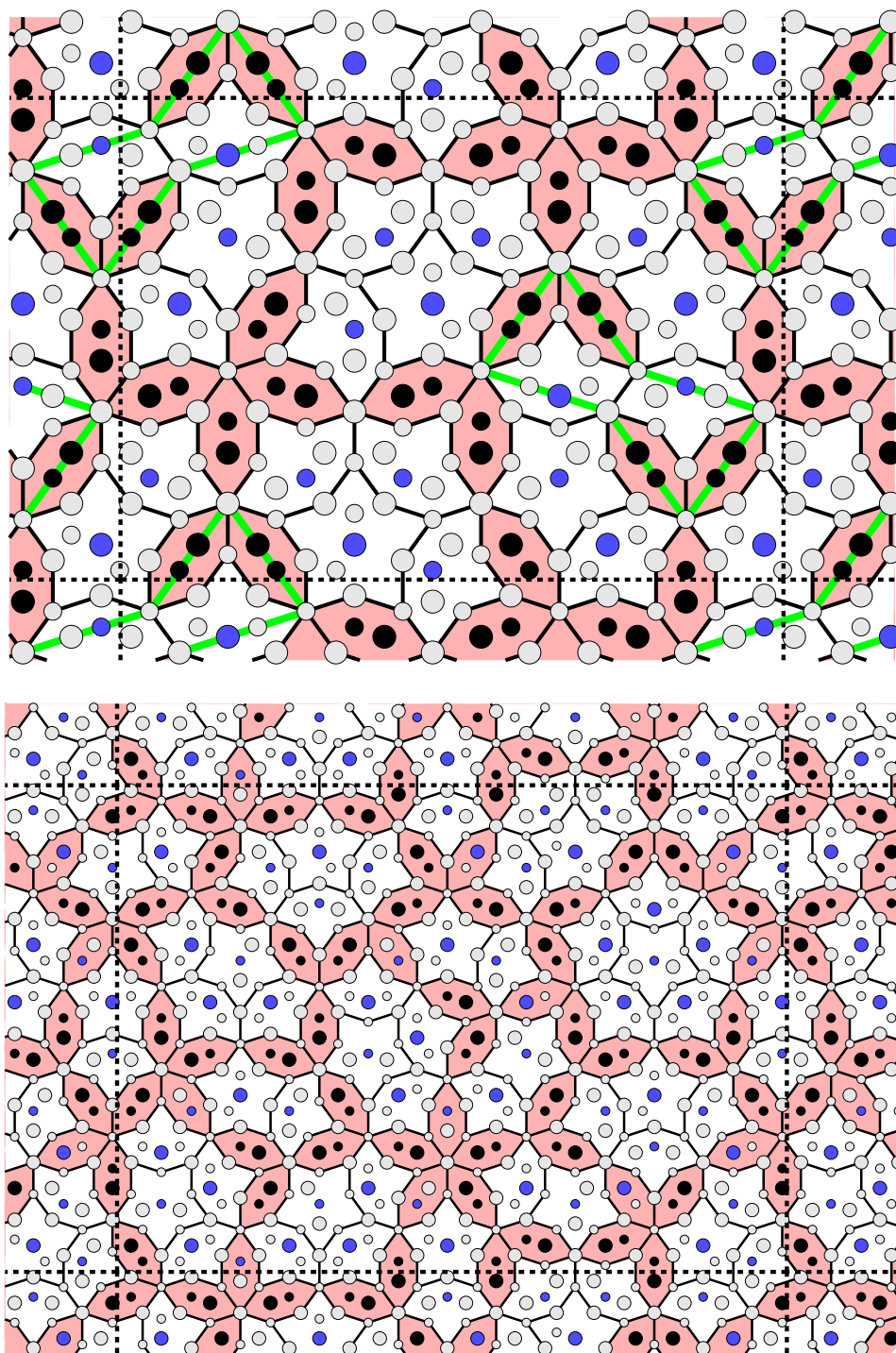


FIG. 3. Lowest energy configurations obtained. (a) Top shows highly constrained simulation. Green lines outline bow tie tiles. (b) Bottom variable occupancy simulation.